

# INTERPOLATION LOGISTIC FUNCTION IN THE SURFACE POTENTIAL BASED MOSFET MODELING

TIJANA KEVKIĆ<sup>1,\*</sup>, VLADICA STOJANOVIĆ<sup>1</sup>

<sup>1</sup>Faculty of Natural Sciences and Mathematics, University of Priština, Kosovska Mitrovica, Serbia

## ABSTRACT

**Introduction of the Interpolation Logistic (IL) function in an approximate Surface-Potential-Based MOSFET model has been proposed in this paper. This function can be precisely determined in accordance with different MOSFET device characteristics. The IL function also provides continual behavior of the surface potential in entire useful region of MOSFET operation. Unlike the approximate analytical models which can meet in literature, continual and smooth transition of the surface potential between weak and strong inversion region here is achieved without using of any empirical parameter. Furthermore, thanks to the IL function, speed and manner of that transition are controlled. The values obtained for the surface potential are verified extensively with the numerical data, and a great agreement is found for the MOSFET devices from different technology generations.**

**Keywords:** MOSFET modeling, Interpolation Logistic function, Surface potential, Parameters estimation.

## INTRODUCTION

Since the choice of a suitable MOSFET model is crucial to the efficiency in the design of both analog and digital integrated circuits, the used model must satisfy some important conditions. First of all, it should reflect the correct physical behavior in order to achieve acceptable accuracy over the required bias conditions. Further, the model must accurately represent device operation over a wide variety of process parameters, geometries and regions of operation. Apart from accuracy, the model used should be as simple as possible in order to limit circuit simulation time.

Among the most accurate physically based MOSFET models are so-called surface potential-based models (henceforth referred to as the SPBM). SPBM fulfill mentioned conditions by the combination of the accuracy of the implicit single-piece models and the short calculation time of regional models (Arora, 1993; Araújo et al., 1995; Prégaldiny et al., 2004). On the other hand, a major difficulty related to these models is an implicit relation between the surface potential  $\psi_s$  and the MOSFET terminal voltages, which needs numerical solutions (Eftimie & Rusu, 2007). Unfortunately, numerical iterative procedures require long computation times what is not desirable from the physical and design point of view (Enz et al., 1995; Chen & Gildenblat, 2001). An attempt to overcome this difficulty is proposed in van Langevelde & Klaassen (2000) as the closed-form approximation for the surface potential. However, that approximation uses for  $\psi_s$  an empirical smoothing function with a smoothing parameter with no physical meaning. Hence, the accuracy of the approximation introduced in van Langevelde & Klaassen (2000) is about 2-3mV which is not always adequate for an accurate modeling of MOSFET characteristics (Hossain & Chowdhury, 2016).

Instead of the empirical smoothing function for  $\psi_s$ , here is proposed a new one that is computationally efficient, well behaved and extremely accurate. This new function is based on the so-called interpolation logistic function which depends on MOSFET devices characteristics. The modified SPBM with proposed new function gives an accurate and continual description of the surface potential in entire inversion region, without any empirical determinations. Finally, the simulated  $\psi_s$  values are compared extensively with numerically obtained results of the mentioned implicit relation and a great agreement was found for MOSFET devices which belong to the different technology generations.

## DEFINITION OF PROBLEM

In the useful range of the n-type MOSFET transistor operation, under the gradual channel and charge sheet approximations, for electrostatic surface potential is obtained the following implicit relation:

$$V_G = V_{FB} + \psi_s + \gamma \sqrt{\psi_s + u_T \exp\left(\frac{\psi_s - 2\phi_F - V_{ch}}{u_T}\right)}. \quad (1)$$

Here  $V_G$ ,  $V_{FB}$  and  $u_T$  are gate voltage, flat-band voltage and thermal voltage, respectively.  $\phi_F$  is bulk potential, while  $V_{ch}$  is the channel potential.  $N_A$  is channel doping concentration,  $t_{ox}$  is thickness of oxide, and  $\gamma$  is body effect coefficient. Numerical solution of Eq.(1) can be obtained by using Newton-Raphson algorithm (Osrečki, 2015). On the other side, the explicit approximate solution of the Eq. (1) developed in van Langevelde & Klaassen (2000)

\* Corresponding author: tijana.kevkic@pr.ac.rs

has following form:

$$\psi_s^*(V_G) = f + u_T \ln \left\{ \gamma^{-2} u_T^{-1} \left[ V_G - V_{FB} - f - \frac{\psi_{s_{wi}} - f}{\sqrt{1 + \left( \frac{\psi_{s_{wi}} - f}{4u_T} \right)^2}} \right]^2 - u_T^{-1} f + 1 \right\}, \quad (2)$$

where

$$\psi_{s_{wi}} = \left( \sqrt{V_G - V_{FB} + \frac{\gamma^2}{4} - \frac{\gamma}{2}} \right)^2 \quad (3)$$

is the surface potential in the weak inversion region and  $f$  is empirical function given by:

$$f(V_G) = \frac{2\phi_F + V_{ch} + \psi_{s_{wi}}(V_G)}{2} - \frac{1}{2} \sqrt{(\psi_{s_{wi}}(V_G) - 2\phi_F - V_{ch})^2 + 4^2}. \quad (4)$$

The value of function  $f$  should changes smoothly from  $\psi_{s_{wi}}$  in the weak inversion region to  $2\phi_F + V_{ch}$  on the onset of the strong inversion region. Smoothness of that transition is controlled by the smoothing parameter which value was firstly fixed at a convenient value of 0.02V (van Langevelde & Klaassen, 2000). Later, it has been replaced with different classes of functions which vary from a value close to zero in depletion and weak inversion region to a value close to 0.02V (Basu & Dutta, 2006; Kevkić et al., 2016, 2017).

However, several simulations have shown that results of Eq. (2) deviate significantly from numerical results of the implicit equation (1). The observed deviations are greater for values of applied gate voltages near and below threshold (i.e., in the weak inversion regime) as well as for scaled MOSFET devices i.e. for devices with thinner gate oxides and higher substrate doping. This is consequence of purely empirical nature of function  $f$ , what means that  $f$  does not take into account changes in specific technology characteristics of the MOSFET devices. Additionally, smoothing parameter does not have physical meaning or role, except to prevent the interruption of the function  $f$  at threshold.

## MODEL FORMULATION

The simple empirical function  $f$ , given by Eq. (4), unifies the weak and strong inversion approximations without inclusion of changes in the technological characteristics of MOSFET devices. In order to take into account mentioned changes and improve description of device behavior, here we suggest the *Interpolation Logistic (IL)* functional form for  $f$ :

$$f_{IL}(V_G) = \psi_{s_{wi}}(V_G) - \frac{u_T}{a} \ln \left[ 1 + b \exp \left( \frac{a}{u_T} (\psi_{s_{wi}}(V_G) - 2\phi_F - V_{ch}) \right) \right]. \quad (5)$$

Here,  $a, b > 0$  are the fitting parameters which can be obtained by using a specific fitting procedure, described in detail in

the following. Notice that in the weak inversion region (i.e., when  $\psi_s < 2\phi_F + V_{ch}$ ), the exponential term in Eq. (5) becomes negligible, so  $f_{IL} \approx \psi_{s_{wi}}$ . On the other side, in the strong inversion region (i.e., when  $\psi_s > 2\phi_F + V_{ch}$ ), the exponential term in Eq. (5) becomes dominant and approximation  $f_{IL} \approx 2\phi_F + V_{ch} + \ln b$  holds. Obviously, term  $\ln b$  can be used to clarify some practically observed deviations from the value  $2\phi_F + V_{ch}$ . It can be easily proven that from the inequalities  $f_{IL}(V_G) \geq 2\phi_F + V_{ch}$  and  $\psi_s > 2\phi_F + V_{ch}$  follows

$$b \leq 1 - \exp \left( -\frac{a}{u_T} (\psi_{s_{wi}}(V_G) - 2\phi_F - V_{ch}) \right) < 1,$$

and vice versa. Therefore, the values of the fitting parameter  $b$  can indicate the changes of the reference  $f$ -values from  $2\phi_F + V_{ch}$ . In particular, if no deviation, i.e., if in the strong inversion region  $f_{IL}(V_G) \approx 2\phi_F + V_{ch}$  holds, it will be  $b \approx 1$ .

The estimation of the fitting parameters  $a, b > 0$  can be done by using the standard fitting procedure based on the following algorithm:

- **Step 1.** For given gate voltage values  $V_G^{(1)}, \dots, V_G^{(n)}$ , numerically solve Eq. (1) with respect to  $\psi_s$ , i.e., compute the values of  $\psi_s^{(1)}, \dots, \psi_s^{(n)}$  such that:

$$V_G^{(k)} - V_{FB} - \psi_s^{(k)} = \gamma \left[ \psi_s^{(k)} + u_T \exp \left( \frac{\psi_s^{(k)} - 2\phi_F - V_{ch}}{u_T} \right) \right]^{1/2}.$$

- **Step 2.** Find values  $f_1, \dots, f_n$  as the solutions of equations  $\psi_s^{(k)} = \psi_s^*(V_G^{(k)})$ ,  $k = 1, \dots, n$ .
- **Step 3.** Minimize the objective function:

$$F(a, b) := \sum_{k=1}^n (f_{IL}(V_G^{(k)}) - f_k)^2$$

with respect to  $a, b > 0$ .

- **Step 4.** For obtained values  $a^*, b^* > 0$  which satisfies  $F(a^*, b^*) = \min F(a, b)$  form the IL-function  $f_{IL}(V_G)$ , as it is given in Eq. (5).

**Table 1.** Estimated values of the  $f_{IL}$ -fitted parameters, according to the MOSFETs technological characteristics.

| Items                        | MOSFET A           | MOSFET B           |
|------------------------------|--------------------|--------------------|
| $t_{ox}$ (nm)                | 2.5                | 1.2                |
| $N_A$ (cm <sup>-3</sup> )    | $5 \times 10^{17}$ | $5 \times 10^{18}$ |
| $\gamma$ (V <sup>1/2</sup> ) | 0.2891             | 0.4494             |
| $2\phi_F$ (V)                | 0.9100             | 1.0416             |
| $V_{FB}$ (V)                 | -0.8000            | -1.0000            |
| $a^*$                        | 1.1638             | 0.9887             |
| $b^*$                        | 1.1737             | 1.1019             |

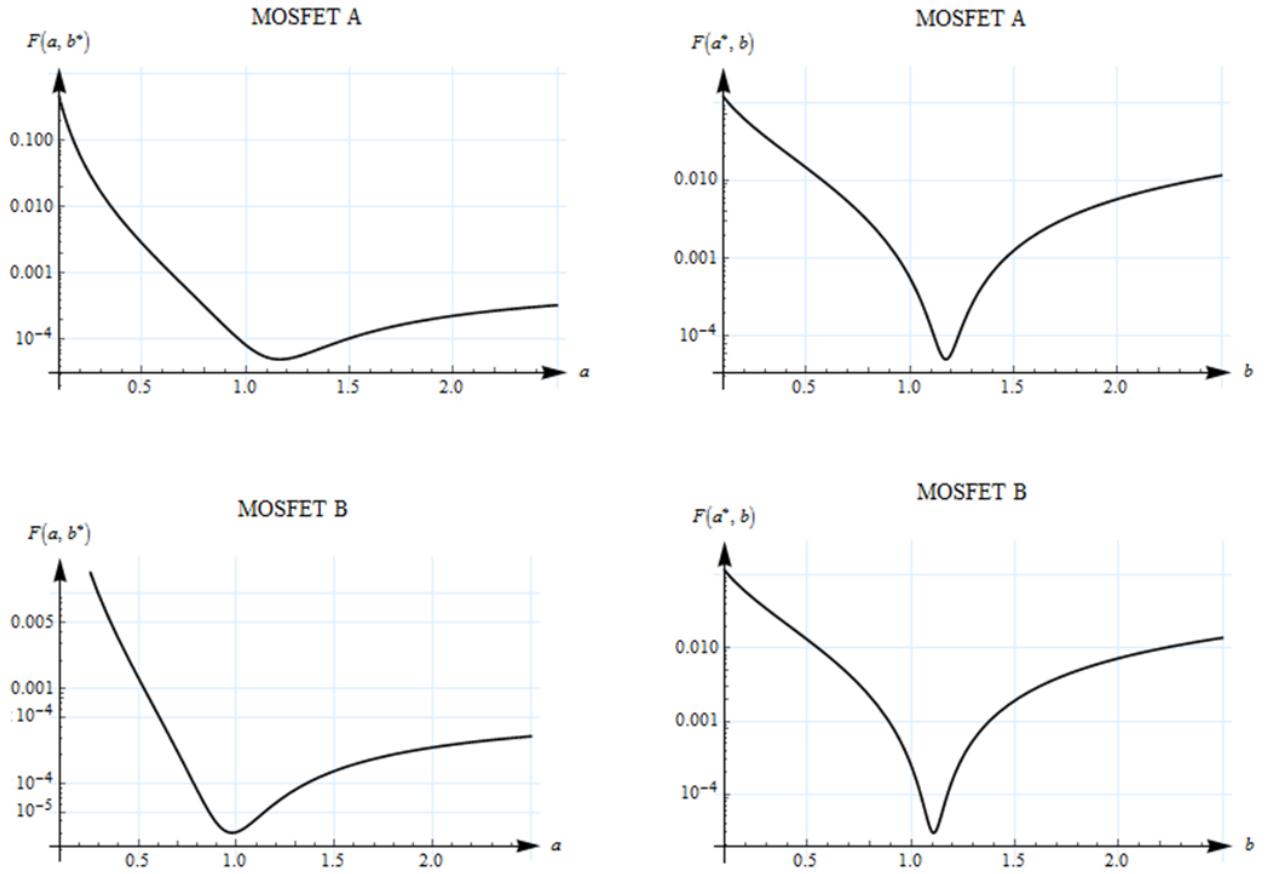


**Figure 1.** Graphs of the objective function  $F(a, b^*)$  (left diagrams) and  $F(a^*, b)$  (right diagrams). Device parameters are: MOSFET A (diagrams above) and MOSFET B (diagrams below).

Notice that minimization of the objective function  $F(a, b)$  in the Step 4 of previous algorithm is performed by using the nonlinear least squared approximate method, i.e., by solving the coupled equations  $\partial F(a, b)/\partial a = \partial F(a, b)/\partial b = 0$ . Estimates of the  $f_{IL}$  parameters  $(a, b) = (a^*, b^*)$  obtained from described algorithm are shown in Table 1, for two MOSFETs with significantly different technological characteristics. All estimates have been obtained based on the series of  $n = 50$  equidistant values of gate voltage  $V_G$ , and the whole algorithm has been implemented in the software package MATHEMATICA 11.0.

Graphs of the functions  $a \mapsto F(a, b^*)$  and  $b \mapsto F(a^*, b)$ , for both of the considered MOSFETs devices are shown in Fig 1. As it can easily be seen, in both cases the function  $F(a, b)$  attains a unique minimum at the point  $(a, b) = (a^*, b^*)$ .

## MODEL VALIDATION

The functions  $f(V_G)$  and  $f_{IL}(V_G)$  are plotted in the above diagrams in Fig. 2 along with the real-based values  $f_1, \dots, f_n$  which were obtained in the Step 2 of previously developed algorithm, and taken as reference values. Diagrams below show approximations of the surface potential  $\psi_s^*(V_G)$ , obtained from Eq. (2), by using both of the functions  $f$  and  $f_{IL}$ , respectively.

The improvement of the original explicit SPB model (van Langevelde & Klaassen, 2000) by introducing the Interpolation

Logistic function can be clearly seen from Tables 2 and 3. They show the mean values of the absolute errors (AE), fractional errors (FE) and squared errors (SE) for functions  $f(V_G)$  and  $f_{IL}(V_G)$ , as the approximate surface potential  $\psi_s^*(V_G)$ . As reference values have been used ones obtained by the previous developed algorithm. For both of considered devices the errors were computed separately in weak and strong inversion region, as well as in the whole approximation region.

As we can see, all the estimated errors are smaller in the case of function  $f_{IL}(V_G)$ , for both of the MOSFETs. This is particularly pronounced in the case of MOSFET A, where for instance, fractional errors which occur in the strong and whole approximation regions are more than six times smaller than corresponding FE value where function  $f$  was used. In the case of MOSFET B, these errors are smaller five times, approximately.

These facts also confirms the Fig. 3 where the absolute errors  $AE = \psi_s^* - \psi_s$  are shown in the logarithmic scales, for both of the mentioned approximations, in the weak and strong inversion, separately. The values of  $\psi_s^*(V_G)$  have been obtained from Eq. (2) by using fitting functions  $f(V_G)$  and  $f_{IL}(V_G)$ , respectively. It is easy to observe that, in all cases, the values of the  $\psi_s^*(V_G)$  with interpolation function  $f_{IL}(V_G)$  show the slightest deviation from reference values.

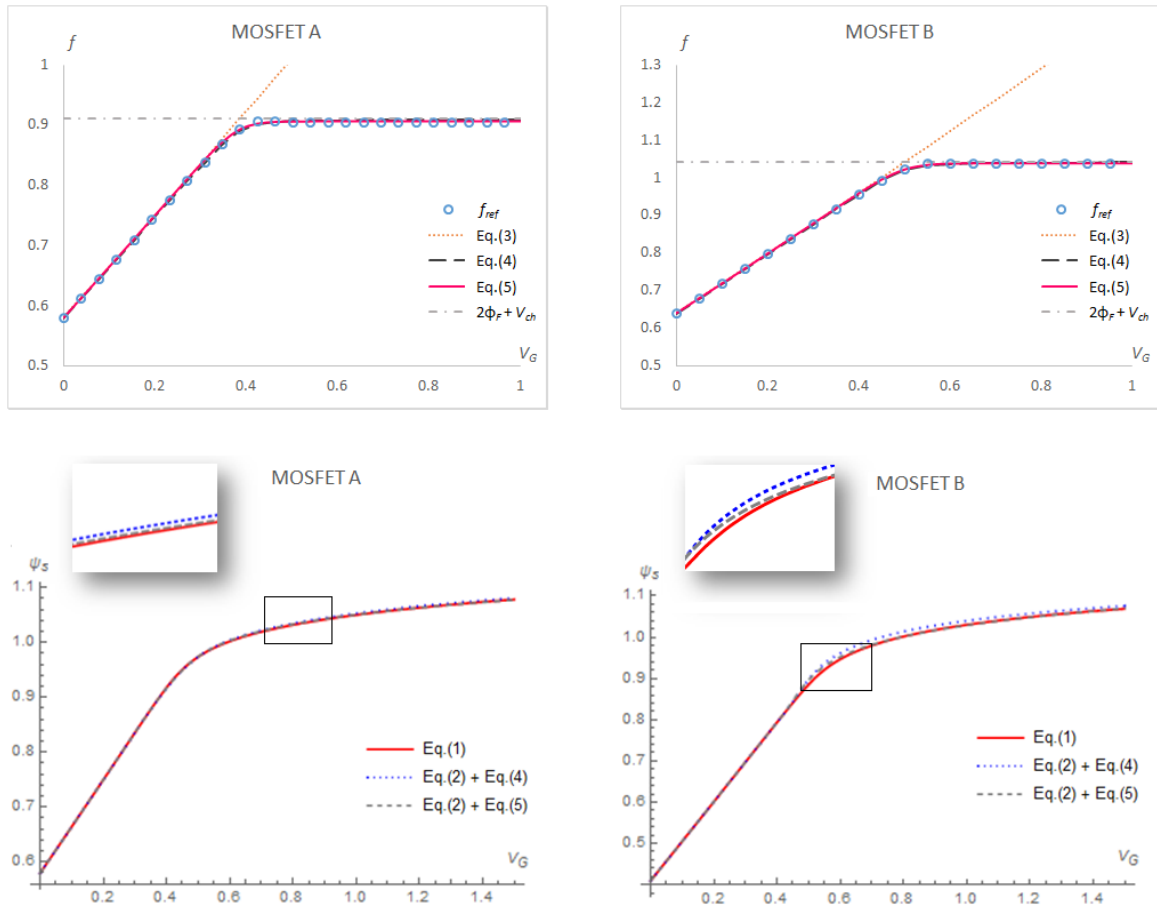


**Figure 2.** Diagrams above: Empirical function  $f(V_G)$  (dashed lines) and interpolation function  $f_{IL}(V_G)$  (solid lines), compared with reference values (dots). Diagrams below: Approximation of the SP using the Eq. (2) with  $f(V_G)$  and  $f_{IL}(V_G)$ . Device parameters are the same as in the MOSFET A (left diagrams) and MOSFET B (right diagrams).

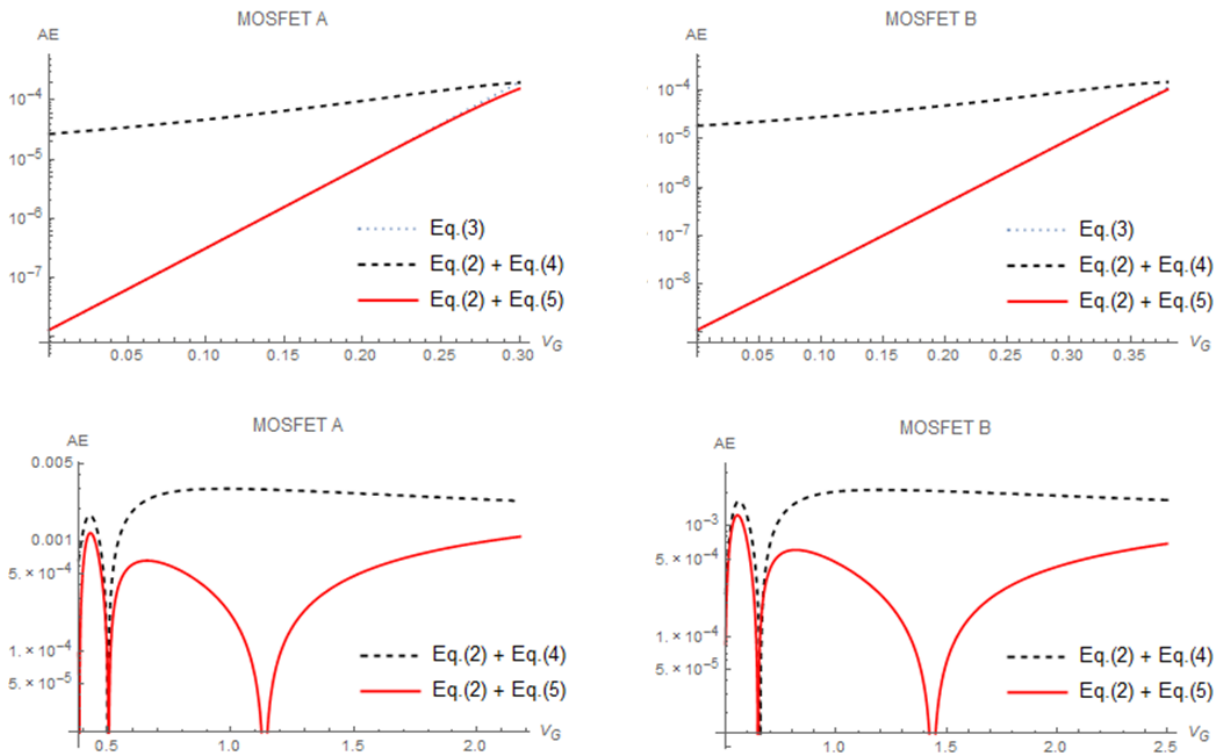


**Figure 3.** Log-diagrams of the absolute errors of the surface potential approximations  $\psi_s^*(V_G)$ , fitted with functions  $f(V_G)$  and  $f_{IL}(V_G)$ , in the the weak inversion (diagrams above), and the strong inversion region (diagrams below).

**Table 2.** Estimated errors obtained by various types of the  $f$ -fitting (MOSFET A).

| Errors   | Regions          | $f$ -fitting |          | $\psi_s^*$ -approximation |          |
|----------|------------------|--------------|----------|---------------------------|----------|
|          |                  | Eq.(4)       | Eq.(5)   | Eq.(4)                    | Eq.(5)   |
| $AE$     | Weak inversion   | 1.53E-03     | 9.73E-04 | 1.07E-04                  | 8.53E-05 |
|          | Strong inversion | 2.97E-03     | 5.59E-04 | 2.47E-03                  | 3.76E-04 |
|          | Whole region     | 2.62E-03     | 6.55E-04 | 1.90E-03                  | 3.05E-04 |
| $FE$ (%) | Weak inversion   | 2.12E-01     | 1.19E-01 | 1.37E-02                  | 9.97E-03 |
|          | Strong inversion | 3.28E-01     | 6.17E-02 | 2.37E-01                  | 3.68E-02 |
|          | Whole region     | 3.00E-01     | 7.52E-02 | 1.83E-01                  | 3.03E-02 |
| $SE$     | Weak inversion   | 2.39E-06     | 2.11E-06 | 1.19E-08                  | 7.03E-09 |
|          | Strong inversion | 9.50E-06     | 8.22E-07 | 6.71E-06                  | 2.06E-07 |
|          | Whole region     | 7.76E-06     | 1.12E-06 | 5.08E-06                  | 1.64E-07 |

**Table 3.** Estimated errors obtained by various types of the  $f$ -fitting (MOSFET B).

| Errors   | Regions          | $f$ -fitting |          | $\psi_s^*$ -approximation |          |
|----------|------------------|--------------|----------|---------------------------|----------|
|          |                  | Eq.(4)       | Eq.(5)   | Eq.(4)                    | Eq.(5)   |
| $AE$     | Weak inversion   | 1.23E-03     | 7.39E-04 | 6.54E-05                  | 2.63E-05 |
|          | Strong inversion | 2.08E-03     | 4.46E-04 | 1.78E-03                  | 3.32E-04 |
|          | Whole region     | 1.84E-03     | 5.14E-04 | 1.36E-03                  | 2.68E-04 |
| $FE$ (%) | Weak inversion   | 1.54E-01     | 7.87E-02 | 7.64E-03                  | 2.79E-03 |
|          | Strong inversion | 2.00E-01     | 4.03E-02 | 1.52E-01                  | 2.89E-02 |
|          | Whole region     | 1.86E-01     | 5.13E-02 | 1.16E-01                  | 2.36E-02 |
| $SE$     | Weak inversion   | 1.71E-06     | 1.40E-06 | 6.26E-09                  | 3.80E-09 |
|          | Strong inversion | 4.66E-06     | 5.20E-07 | 3.43E-06                  | 1.73E-07 |
|          | Whole region     | 7.76E-06     | 1.12E-06 | 2.60E-06                  | 1.38E-07 |

## CONCLUSIONS

Implementation of the Interpolation Logistic function in explicit surface potential based MOSFET model is described. This function provides continual transition of the surface potential between two distinct regions of MOSFET operation and simultaneously controls speed and manner of that transition. Except the need for usage of any empirical functions or parameters with no physical meaning is eliminated, by introducing the proposed function is achieved significantly higher degree of accuracy for the surface potential over a wide range of the device parameters. Moreover, the complexity of the calculations increases only marginally over the original model which contains pure empirical function for surface potential.

## REFERENCES

Araújo, C. A. I., Schneider, M. C., & Galup-Montoro, C. 1995. An explicit physical model for the long-channel MOS transistor including small-signal parameters. *Solid-State Electronics*, 38(11), pp. 1945-1952. doi:10.1016/0038-1101(95)00023-m.

Arora, N. 1993. *MOSFET Models for VLSI Circuit Simulation*. Vienna: Springer-Verlag. doi:10.1007/978-3-7091-9247-4.

Basu, D. & Dutta, A. 2006. An explicit surface-potential-based MOSFET model incorporating the quantum mechanical effects. *Solid-State Electron.*, 50, pp. 1299-1309.

Chen, T. L. & Gildenblat, G. 2001. Analytical approximation for the MOSFET surface potential. *Solid-State Electronics*, 45(2), pp. 335-339. doi:10.1016/s0038-1101(00)00283-5.

Eftimie, S. & Rusu, A. 2007. MOSFET model with simple extraction procedures suitable for sensitive analog simulations. *Rom. J. Inf. Sci. Tech.*, 10, pp. 189-197.

Enz, C., Krummenacher, F., & Vittoz, E. 1995. An analytical MOS transistor model valid in all regions of operation and dedicated to low-voltage and low-current applications. *Analog Integrated Circuits and Signal Processing*, 8(1), pp. 83-114. doi:10.1007/bf01239381.

Hossain, M. & Chowdhury, M. 2016. Comprehensive doping scheme for MOSFETs in ultra-low-power subthreshold circuits design. *Microelectronics Journal*, 52, pp. 73-79. doi:10.1016/j.mejo.2016.03.007.

- Kevkić, T., Stojanović, V., & Joksimović, D. 2017. Application of generalized logistic functions in surface-potential-based MOSFET modeling. *Journal of Computational Electronics*, 16(1), pp. 90-97. doi:10.1007/s10825-016-0935-x.
- Kevkić, T., Stojanović, V., & Petković, D. 2016. Modification of transition's factor in the compact surface-potential-based MOSFET model. *The University Thought - Publication in Natural Sciences*, 6(2), pp. 55-60. doi:10.5937/univtho6-11360.
- Osrečki, Z. 2015. Compact MOSFET model. University of Zagreb. Thesis.
- Prégaldiny, F., Lallement, C., van Langevelde, R., & Mathiot, D. 2004. An advanced explicit surface potential model physically accounting for the quantization effects in deep-submicron MOSFETs. *Solid-State Electronics*, 48(3), pp. 427-435. doi:10.1016/j.sse.2003.09.005.
- van Langevelde, R. & Klaassen, F. 2000. An explicit surface-potential-based MOSFET model for circuit simulation. *Solid-State Electronics*, 44(3), pp. 409-418. doi:10.1016/s0038-1101(99)00219-1.